Characterization of amorphous Si generated through classical molecular dynamics simulations

Iván Santos*†, Pedro López*, María Aboy*, Luis A. Marqués* and Lourdes Pelaz*

*Departamento de Electricidad y Electrónica, E.T.S.I. Telecomunicación, Universidad de Valladolid

Paseo Belén 15, 47011 Valladolid, Spain

†Corresponding author: ivasan@tel.uva.es, (+34) 983 423683 ext. 5512

***Abstract*—We performed a characterization of the energetic and structural features of amorphous Si using classical molecular dynamics simulations. We generated amorphous Si samples from different procedures: quenching liquid silicon, accumulating the damage generated by subsequent energetic recoils, and accumulating point defects. The obtained energetic and structural features of these types of samples are analyzed to elucidate which procedure provides a more realistic a-Si structure.**

I. Introduction

Amorphous silicon (*a*-Si) is widely used in inexpensive high efficient heterojunction and thin-film solar cells [1]. Further enhancements need from fundamental studies of phenomena limiting the efficiency [2], [3]. Amorphous Si can be also intentionally generated during doping of crystalline Si (*c*-Si) to improve dopant activation [4], but the changes in its structure during annealing greatly affects dopant diffusion [5]. A proper description of the underlying amorphous matrix is necessary to understand these effects, but this is not a simple task as *a*-Si lacks of a defined structure. The structure and properties of *a*-Si depend on how it is generated [6]–[9]. Its relaxation state is directly related to its energy and bond angle dispersion ($\Delta\theta$), parameters commonly used for its characterization [7]. Amorphous Si generated by ion implantation is highly unrelaxed, with an energy of ~ 0.19 eV/atom above *c*-Si and $\Delta\theta \sim 11°$. Relaxed *a*-Si has an energy of ~ 0.14 eV/atom and $\Delta\theta \sim 9°$. Theoretical static models were also developed to describe the structure of fully relaxed *a*-Si. The so called *WWW* model results in energies of 0.23 eV/atom and $\Delta\theta \sim 11°$ [9], [10], and the *BM* model in energies of 0.22 eV/atom and $\Delta\theta \sim 10°$ [11]. Atomistic simulations of atom dynamics can also be used to generate *a*-Si. Classical molecular dynamics simulations offer a good balance between computational cost, system size, and simulation time. One of the most difficult issues is to generate realistic amorphous samples. In this paper, we analyze three different procedures to generate *a*-Si samples using classical molecular dynamics simulations. We generated *a*-Si samples from quenching liquid Si (*l*-Si), from the accumulation of damage generated by recoils, and from the accumulation of point defects. We evaluated the energetics and structural features of generated samples

for comparison with known features of *a*-Si.

II. Simulation details

We used the empirical potential developed by Tersoff in its third parametrization to describe the interactions among Si atoms [12]. It adequately describes the structural properties of point defects in *c*-Si [13], and of *a*-Si [14], [15]. It was used to study the formation of *a*-Si by quenching *l*-Si [14], and different phenomena related to ion irradiation in *c*-Si [16]. The simulation cells employed had 576 atoms, and we applied periodic boundary conditions in all spatial directions.

We generated *a*-Si using different procedures. The first type of *a*-Si was obtained by quenching *l*-Si. This is a common procedure to obtain *a*-Si using molecular dynamics simulations [14] that resembles the preparation of *a*-Si by laser techniques (fast melting of *c*-Si by laser illumination, followed by quenching of the obtained *l*-Si into *a*-Si). We melted *c*-Si by heating it to 4000 K. The obtained *l*-Si was quenched to 300 K with cooling rates from $7.8 \cdot 10^{12}$ to $8.4 \cdot 10^{14}$ K/s.

The second type of *a*-Si was generated by accumulating the damage generated by energetic recoils, which resembles the generation of *a*-Si by ion implantation. We sequentially initiated 100 independent 200 eV recoils in random directions applied to randomly selected atoms, and we set the initial temperature of the simulation cell to 0 K. The evolution of cascades was followed during 5 ps, time long enough to encompass the recoil dynamics. Then, atom coordinates were averaged during 1 ps. Averaged atomic positions were used as the initial configuration for the next recoil so damage kept accumulating.

A third type of *a*-Si was generated by point defect accumulation. In the critical point defect density model, Si amorphization is envisioned as a phase transition induced by the accumulation of a critical defect concentration in *c*-Si [17]. We considered in our study the accumulation of the so called *bond defect*. This defect has no excess or deficit of atoms but it introduces disorder in the Si lattice [18], [19]. Bond defects can be primary defects generated by irradiation [20], and the amorphization of *c*-Si can also be achieved by the accumulation of bond defects [19]. In our study, we introduced two different concentrations of bond defects in *c*-Si at random positions. In one sample we tried to introduce the maximum concentration of bond defects. Theoretically it is equal to 50 % as bond defects are formed by two Si atoms, but only 45 % was achieved as not all possible positions are selected due to geometrical constrains in the random placing of bond defects. In the other sample, we introduced 30 % of bond defects, which is the minimum concentration at which a simulation cell remains amorphous during thermal annealing at any temperature [19]. We will refer to these samples as BDH and BDL for the higher and lower concentrations, respectively.

Samples obtained from the procedures previously described were thermalized at 300 K during 10 ps using velocity rescaling. Atom positions and energies were averaged in the last 5 ps for the characterization of generated samples. We used a distance of 2.85 Å for identifying nearest neighbors of atoms.

III. Results and discussion

We evaluated the following parameters for the structural characterization of generated *a*-Si samples: atomic coordination, potential energy per atom with respect to *c*-Si, percentage of Si atoms with three (n_3), four (n_4), five (n_5) and six (n_6) Si neighbors, average bond length and its dispersion, and average bond angle and its dispersion. Obtained results are shown in Fig. 1 for quenched *a*-Si as

a function of the cooling rate (shown results correspond to samples equilibrated at 300 K), in Fig. 2 for samples generated by recoils as a function of the recoil number (shown results correspond to samples just after the stop of the recoil, i.e. samples are not thermalized at 300 K), and in Table I for *a*-Si samples generated by bond defect accumulation after equilibration at 300 K.

Experiments show that relaxed *a*-Si has atomic coordination close to 4, energy of $\sim$ 0.1 eV/atom over *c*-Si, bond angles close to 109.5°, and $\Delta\theta \sim 9°$. On the other hand, unrelaxed samples have higher atomic coordination and energy, average bond angle smaller than 109.5°, and a higher value of $\Delta\theta$ [6]–[9]. According to these observations, our results indicate that slower cooling rates increase the relaxation state of the generated *a*-Si sample, in agreement with previous studies [14]. In addition, more relaxed *a*-Si samples have a larger percentage of fourfold Si atoms, which would be ideally 100% in a perfectly relaxed sample. For *a*-Si generated by recoils, Fig. 2 shows two different stages with a clear variation of properties above and below $\sim$ 40 recoils. As damage is being accumulated, the sample evolves towards a more unrelaxed state that corresponds to the damage accumulation in the initial *c*-Si sample. Once

TABLE I

ENERGETIC AND STRUCTURAL FEATURES OF *a*-SI SAMPLES GENERATED BY BOND DEFECT ACCUMULATION

Sample	**BDL**	**BDH**
Bond defect concentration	30%	45%
Potential energy (eV/atom)	0.39	0.43
Atomic coordination	4.2	4.3
Three-fold coordinated Si atoms, n_3	4.3%	3.8%
Four-fold coordinated Si atoms, n_4	74.1%	66.0%
Five-fold coordinated Si atoms, n_5	19.6%	28.1%
Six-fold coordinated Si atoms, n_6	1.9%	2.1%
Average bond length (Å)	2.40	2.42
Bond length dispersion (Å)	0.09	0.09
Average bond angle (°)	107.9	107.4
Bond length dispersion (°)	18.6	20.5

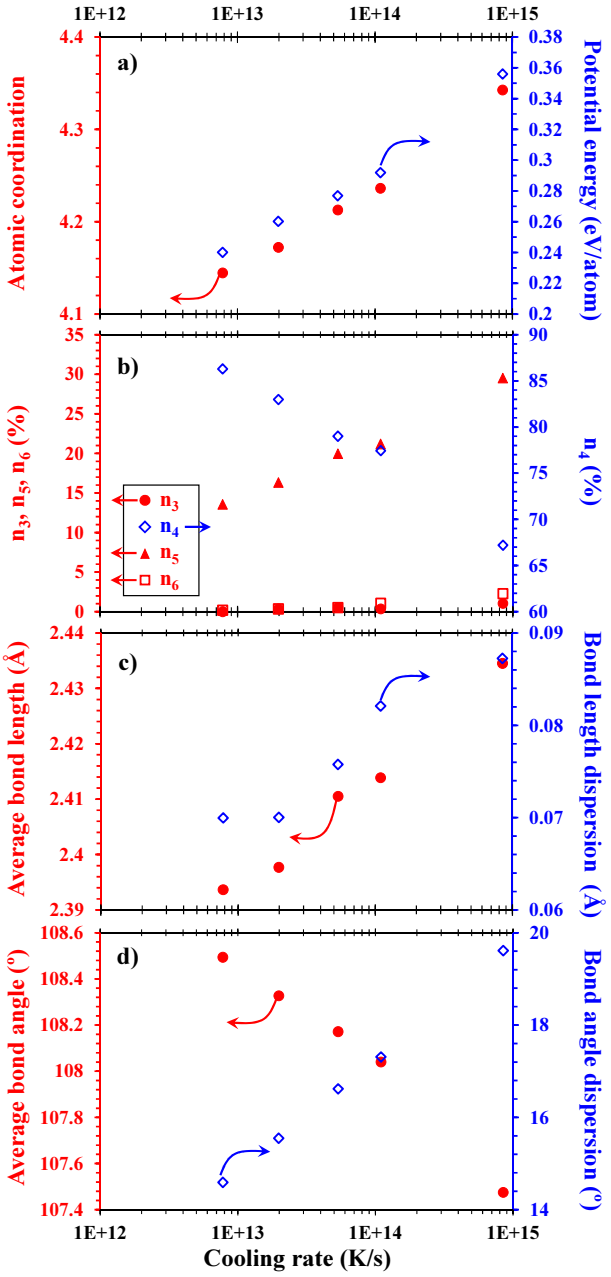

Fig. 1. Energetic and structural features for quenched *a*-Si samples as a function of the cooling rate.

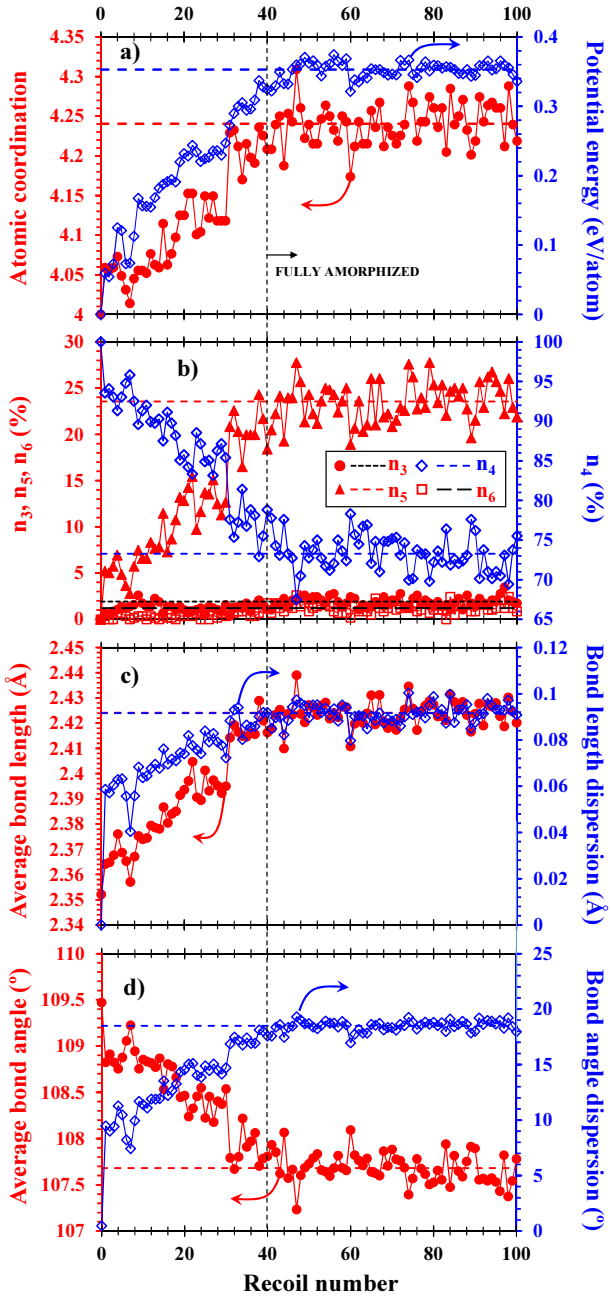

Fig. 2. Energetic and structural features for samples generated by recoils as a function of the recoil number. Horizontal dashed lines show the average final values of represented magnitudes. Vertical dashed line marks the amorphization of the sample.

the sample is fully amorphized, its properties reach a stationary state that is not modified by additional recoils. The resulting *a*-Si is highly unrelaxed. Finally, Table I shows that lower defect concentrations of bond defects (30%) result in more relaxed *a*-Si samples, but generated samples are highly unrelaxed for both concentrations of bond defects.

Obtained results suggest correlations between the analyzed energetic and structural features in *a*-Si. To highlight these correlations, we represented in Fig. 3 the atomic coordination as a function of the potential energy per atom in the generated *a*-Si samples. For *a*-Si generated by recoils, we show the properties of as implanted samples once the cell is fully amorphized (open squares), the average properties of the amorphized sample (solid triangle), and the properties of the sample after the last recoil equilibrated at 300 K (open triangle). It can be seen that quenched *a*-Si shows a linear trend: the lower the potential energy, the lower the atomic coordination. This trend agrees with experimental results as previously mentioned [7], [8]. In addition, quenched *a*-Si constitutes a limit to other *a*-Si samples as it has the lower potential energy for each atomic coordination. Samples generated by recoils have higher potential energy for the same atomic coordination, but fall in the trend of quenched *a*-Si after equilibration at 300 K. Samples generated by bond defect accumulation have the highest energies. We represented in Fig. 4 the average bond angle and its dispersion as a function of the potential energy for the *a*-Si samples equilibrated at 300 K. As in Fig. 3, quenched *a*-Si samples and *a*-Si generated by recoils equilibrated at 300 K follow a linear trend that agrees with experimental observations: more relaxed *a*-Si samples present bond angles closer to 109.5° and a lower $\Delta\theta$. Samples generated by bond defect accumulation fall out this trend, and show low average bond angles and high $\Delta\theta$ corresponding to highly unrelaxed *a*-Si.

We also evaluated the radial distribution function,

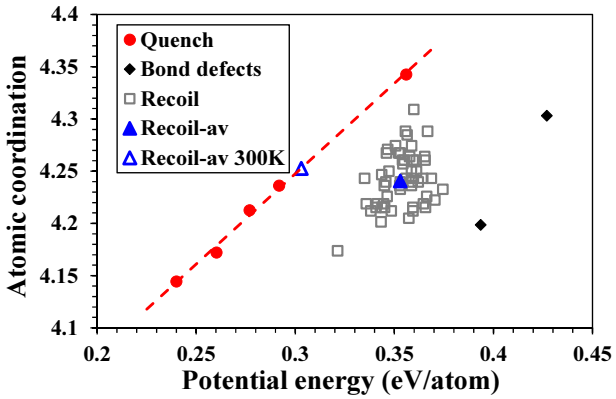

Fig. 3. Atomic coordination as a function of the potential energy in the *a*-Si samples generated (see text for details). Dashed line is to guide the eye.

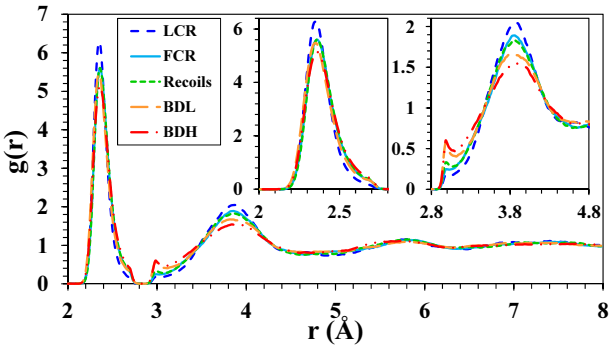

Fig. 5. Radial distribution function for *a*-Si samples generated with the lowest (LCR) and fastest cooling rates (FCR), with recoils (equilibrated at 300 K) and with bond defect accumulation. Insets magnify selected zones for a better comparison.

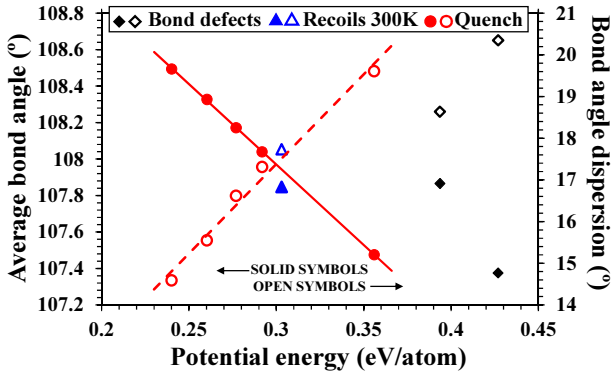

Fig. 4. Average bond angle and $\Delta\theta$ as a function of the potential energy for the *a*-Si samples equilibrated at 300 K. Straight lines are to guide the eye.

which is we represented in Fig. 5 for selected *a*-Si samples. It can be seen that quenched *a*-Si with the slowest cooling rate considered ($7.8 \cdot 10^{12}$ K/s) shows the highest first peak, and the lowest values in the region between the first and the second peaks. These facts are related to a more relaxed structure. The sample generated by recoils has a pair correlation function similar to the quenched *a*-Si with the fastest cooling rate ($8.4 \cdot 10^{14}$ K/s), which indicates a less relaxed structure. Finally, samples generated by accumulation of bond defects present a pair correlation function of highly unrelaxed *a*-Si: a lower first peak in the radial distribution function, a wider second peak, and higher values in the region between the first and the second peaks. Weak peaks at the sides of the empty region around 2.8 Å are known effects due to the cut-off function in the empirical potential [12].

Thus, the more relaxed *a*-Si sample is achieved by quenching *l*-Si with the slowest cooling rate considered ($7.8 \cdot 10^{12}$ K/s). While its energy (0.24 eV/atom) is comparable to the obtained by other theoretical models, its structural characteristics are still far from well relaxed *a*-Si: high atomic coordination (4.14), low average bond angle (108.5°), and high bond angle dispersion ($\Delta\theta = 14.6°$). A logarithmic fit of data shown in Fig. 1 indicates that a cooling rate of $\sim 4.3 \cdot 10^{10}$ K/s would result in a potential energy of ~ 0.11 eV, a bond angle of $\theta \sim 109.6°$, $\Delta\theta \sim 9°$, and an atomic coordination of 3.91. Thus, the generation of *a*-Si by quenching *l*-Si with a cooling rate of $\sim 4.3 \cdot 10^{10}$ K/s would potentially result in a highly relaxed sample. Nevertheless, the slowest cooling rate achieved by molecular dynamics simulations up to now is 10^{11} K/s to the authors' knowledge [21], and thus the expected features need to be confirmed with a real simulation.

IV. Conclusions

We analyzed the efficiency of generating realistic samples of *a*-Si from quenching *l*-Si, from the accumulation of damage generated by recoils, and from the accumulation of bond defects using classical molecular dynamics simulations. For this purpose, we correlated the energetic and structural features of generated *a*-Si samples with their relaxation state. We found that quenching *l*-Si is the best procedure for generating *a*-Si among the ones analyzed. Quenched samples had the lower potential energy for each possible atomic coordination. The more relaxed *a*-Si sample achieved was generated by quenching *l*-Si with the slowest cooling rate considered, but its features are far from the expected ones for well relaxed *a*-Si. Nevertheless, cooling rates of $\sim 4.3{\cdot}10^{10}$ K/s are expected to generate a highly relaxed *a*-Si sample, which will be investigated in future work.

Acknowledgment

This work has been supported by EU (FEDER) and the Spanish Ministerio de Ciencia e Innovación under Project No. TEC2014-60694-P, and by the Junta de Castilla y León under Project No. VA331U14.

References

[1] H. Sai, T. Matsui, and K. Matsubara. "*Stabilized 14.0%-efficient triple-junction thin-film Si solar cell*," Appl. Phys. Lett. **109**, 183506 (2016)

[2] L. K. Wagner and J. C. Grossman. "*Microscopic Description of Light Induced Defects in Amorphous Si Solar Cells*," Phys. Rev. Lett. **101**, 265501 (2008)

[3] I. Santos, *et al.* "*Self-trapping in B-doped amorphous Si: Intrinsic origin of low acceptor efficiency*," Phys. Rev. B **81**, 033203 (2010)

[4] M. Canino, *et al.* "*Defect engineering via ion implantation to control B diffusion in Si*," Mat. Sci. Eng. B **159–160**, 338 (2009)

[5] S. Mirabella, *et al.* "*Mechanism of Boron Diffusion in Amorphous Silicon*," Phys. Rev. Lett. **100**, 155901 (2008)

[6] S. Roorda, *et al. "Structural relaxation and defect annihilation in pure amorphous silicon,"* Phys. Rev. B **44**, 3702 (1991)

[7] P. Roura, *et al. "Quantification of the bond-angle dispersion by Raman spectroscopy and the strain energy of a-Si,"* J. Appl. Phys. **104**, 073521 (2008)

[8] P. A. Stolk, *et al. "Contribution of defects to electronic, structural, and thermodynamic properties of a-Si,"* J. Appl. Phys. **75**, 7266 (1994)

[9] E. Holmström, *et al. "Dependence of short and intermediate-range order on preparation in experimental and modeled pure a-Si,"* J. Non-Cryst. Solids **438**, 26 (2016)

[10] F. Wooten, K. Winer, and E. Weaire. "*Computer Generation of Structural Models of Amorphous Si and Ge*," Phys. Rev. Lett. **54**, 1392 (1985)

[11] R. L. C. Vink, *et al.* "*Device-size atomistic models of amorphous silicon*," Phys. Rev. B **64**, 245214 (2001)

[12] J. Tersoff. "*Empirical interatomic potential for silicon with improved elastic properties*," Phys. Rev. B **38**, 9902 (1988)

[13] L. A. Marqués, L. Pelaz, P. Castrillo, and J. Barbolla. *"Molecular dynamics study of the configurational and energetic properties of the silicon self-interstitial,"* Phys. Rev. B **71**, 085204 (2005)

[14] M. Ishimaru, S. Munetoh, and T. Motooka. *"Generation of amorphous silicon structures by rapid quenching: A molecular-dynamics study,"* Phys. Rev. B **56**, 15133 (1997)

[15] L. A. Marqués, L. Pelaz, M. Aboy, and J. Barbolla. *"The laser annealing induced phase transition in silicon: a molecular dynamics study,"* Nucl. Instrum. Meth. B **216**, 57 (2004)

[16] K. M. Beardmore and N. Grønbech-Jensen. *"Direct simulation of ion-beam-induced stressing and amorphization of Si,"* Phys. Rev. B **60**, 12610 (1999)

[17] G. Hobler and G. Otto. *"Status and open problems in modeling of as-implanted damage in silicon,"* Mat. Sci. Semicon. Pro. **6**, 1 (2003)

[18] M. Tang, L. Colombo, J. Zhu, and T. Diaz de la Rubia. *"Intrinsic point defects in crystalline silicon: Tight-binding molecular dynamics studiesof self-diffusion, interstitial-vacancy recombination, and formation volumes",* Phys. Rev. B **55**, 14279 (1997)

[19] L. A. Marqués, *et al. "Stability of defects in crystalline silicon and their role in amorphization,"* Phys. Rev. B **64**, 045214 (2001)

[20] D. M. Stock, B. Weber, and K. Gärtner. *"Role of the bond defect for structural transformations between crystalline and amorphous silicon: A molecular-dynamics study,"* Phys. Rev. B **61**, 8150 (2001)

[21] D. Choudhary, and P. Clancy. *"Characterizing the nature of virutal a-Si,"* J. Chem. Phys. **122**, 174509 (2005)